Drug Development and Industrial Pharmacy

http://informahealthcare.com/ddi
ISSN: 0363-9045 (print), 1520-5762 (electronic)

Drug Dev Ind Pharm, Early Online: 1–9
 DOI: 10.3109/03639045.2013.858737

informa
healthcare

RESEARCH ARTICLE

Spray drying formulation of albendazole microspheres by experimental design. *In vitro–in vivo* studies

Agustina García[1,2], Darío Leonardi[1,2], Gisela N. Piccirilli[1,3], María E. Mamprin[4], Alejandro C. Olivieri[1,3], and María C. Lamas[1,2]

[1]*IQUIR – CONICET,* [2]*Área Técnica Farmacéutica,* [3]*Área Química Analítica, and* [4]*Área Farmacología, Facultad de Ciencias Bioquímicas y Farmacéuticas, UNR, Suipacha 531, Rosario, Argentina*

Abstract

Both an experimental design and optimization techniques were carried out for the development of chitosan–pectin–carboxymethylcellulose microspheres to improve the oral absorption of albendazole as a model drug. The effect of three different factors (chitosan, pectin and carboxy methyl cellulose concentrations) was studied on five responses: yield, morphology, dissolution rate at 30 and 60 min, and encapsulation efficiency of the microspheres. During the screening phase, the factors were evaluated in order to identify those which exert a significant effect. Simultaneous multiple response optimizations were then used to find out experimental conditions where the system shows the most adequate results. The optimal conditions were found to be: chitosan concentration, 1.00% w/v, pectin concentration 0.10% w/v and carboxymethylcellulose concentration 0.20% w/v. The bioavailability of the loaded drug in the optimized microspheres was evaluated in Wistar rats which showed an area under curve (AUC) almost 10 times higher than the pure drug.

Keywords

Albendazole, biomaterials, microspheres, oral drug release, spray drying

History

Received 28 June 2013
Revised 3 October 2013
Accepted 4 October 2013
Published online 18 November 2013

Introduction

In the last decades, natural polysaccharides and their derivatives have been widely used as carriers for developing the drug delivery systems due to their useful characteristics including biocompatibility, biodegradability, pH sensitivity and mucoadhesive property. Specifically, intermolecular interactions between polysaccharides of opposite charge lead to the formation of polyelectrolyte complexes (PECs)[1–6].

In this context, the concept of PECs has been applied to the design of drug delivery systems due to the non-toxic and biocompatible properties of the PECs components. As described in the literature, one of the advantages of PECs is their ability to encapsulate active compounds in the polymeric matrix at molecular level, altering physicochemical properties of the active molecules, such as solubility, dissolution stability and pharmacokinetic properties[7–9]. It is well documented that microparticulate systems prepared by means of PECs offer numerous advantages over traditional methods of drug delivery, including tailoring of drug release rates[10], protection of fragile drugs[11] and increased patient comfort and compliance[12]. One of the most common polysaccharides used for the PECs formation is chitosan (CH), a cationic polymer obtained from the alkaline deacetylation of chitin, the principal component of the cuticles of crabs and shrimps, fungus cells walls and insect cuticles. It is a copolymer composed of β (1 → 4)-linked 2-amino-2-deoxy-D-glucopyranose units and 2-acetamido-2-deoxy-D-glucopyranose units. CH has attracted increasing attention due to their favorable properties including biocompatibility, biodegradability and mucoadhesivity[13–16]. In acid medium, the positive-charged amino groups on the C2 position of CH may react with an anionic group of other polymers leading to the generation of PECs[17]. One of the polymers with the capability of reacting with CH is pectin (P), a natural polyanion found in the primary cell walls and middle lamella of dicotyledonous plants. In the last years, the properties of PECs composed of CH and P have been extensively investigated for the preparation of colon-specific drug delivery systems[18–21].

One of the advantages of PEC microencapsulation methodology is attributed to its mild condition without the application of potentially toxic organic solvents, as opposed to other delivery systems[22,23].

On the other hand, sodium carboxymethylcellulose (CMC) which is a linear, long-chain, water-soluble, anionic polysaccharide is found in the fibrous tissue. It is an important cellulose derivative primarily due to its high viscosity, non-toxicity and non-allergic properties with applications, among others, in the pharmaceutical, food, paper and textile industries. It has also been used to form PECs with CH through the interaction of the positively charged amino group of CH and the negatively charged carboxylate group of the cellulose derivative, at the appropriate pH. Complexes of CH with CMC have been evaluated as a tool for drug delivery in order to provide the required physicochemical properties for the design of specific drug delivery systems[24,25].

Albendazole (ABZ), methyl (5-[propylthio]-1 H-benzimidazol-2-yl) carbamate, a benzimidazole derivative was selected as a model drug, which is poorly soluble in water (1 μg/mL). It is included into Class II of the Biopharmaceutical Classification

Address for correspondence: María C. Lamas, Facultad de Ciencias Bioquímicas y Farmacéuticas, Suipacha 531 – (2000) Rosario, Argentina. Tel: +54-341-4804592. Fax: +54-341-4370477. E-mail: mlamas@fbioyf.unr.edu.ar

System, since its low solubility is a major obstacle in the development of oral solid dosage form with appropriate biopharmaceutical properties[26,27]. As already described, the dissolution characteristics of ABZ represent a great challenge because they are the rate-limiting in the drug absorption process after oral administration[28]. Several attempts to increase the aqueous solubility/dissolution rate of ABZ by means of freeze-drying, spray-drying, ionic gelation and emulsification with or without cross-linking agents have been reported[29–33]. However, there is no information available about *in vitro*/*in vivo* performance of ABZ encapsulated into microspheres of CH-based PECs prepared with P and CMC.

Therefore, the aim of this work was to study the production of ABZ–PEC–microspheres using the spray-drying methodology. Experimental design and specific response surface analysis[34–36] were applied to improve the properties of the ABZ formulations.

The effect of three factors (CH, P and CMC concentrations) was evaluated, in order to distinguish those which have a significant effect on five responses: yield (*Y*), morphology (*M*), encapsulation efficiency (*EE*) and dissolution rate at 30 (Q_{30}) and 60 (Q_{60}) min. In addition, the bioavailability of the optimal formulation was evaluated as compared to the untreated drug.

Materials and methods

Materials

ABZ, P ($M_W > 180$ kDa) and sodium CMC ($M_W > 250$ kDa) were supplied by Sigma-Aldrich Chemie GmbH (Steinheim, Germany) and CH by Aldrich Chemical Co. ($M_W > 300$ kDa, degree of deacetylation >85%) (Milwaukee, WI). All other chemicals were of analytical grade.

Methods

Preparation of ABZ–CH microspheres

Microspheres were prepared by the spray-drying method, performed according to the following procedure: ABZ (100 mg) was dissolved at room temperature in glacial acetic acid and distilled water was added to obtain a concentration of 30% v/v. A given amount of CH was dispersed in the acetic acid solution. CMC and P solutions were prepared by dissolving in 100 mL of water and stirred for 2 h. The concentrations of the polymer solutions depended on the experimental design (Tables 1 and 2). The polymer solutions were heated at 45 °C and then the binary system CMC-P was slowly dropped over ABZ–CH solution, avoiding the aggregate formation. The spray-drying conditions were in accordance with Piccirilli et al.[37]. The spraying procedure was carried out with a Mini Spray Dryer Buchi B-290 (Flawil, Switzerland). The following parameters remained constant: airflow rate 38 m^3/h, feed rate 5 mL/min and aspirator set at 100%. The spray-drying inlet temperature was set at 130 °C; the outlet temperature was recorded at 70 °C.

Characterization

The yield (*Y*), *EE* and dissolution profiles were performed in accordance with Leonardi et al.[35].

Yield determination

The yield (*Y*) was calculated as the ratio between the experimental weight of product and the sum of the weights of all components:

$$Y(\%) = 100 \times \left[W_{\text{product}}/(W_{\text{ABZ}} + W_{\text{CH}} + W_{\text{P}} + W_{\text{CMC}})\right] \quad (1)$$

where W_{product} is the weight of the obtained microspheres and W_{ABZ}, W_{CH}, W_{P} and W_{CMC} are the weights of ABZ and ionic polymers, respectively.

Table 1. Plackett–Burman design.

Run	P % w/v	CH % w/v	CMC % w/v	*Y* (%)	Q_{30} (%)	Q_{60} (%)	*EE* (%)
1	0.00	1.00	0.00	100	58.0	67.4	83.93
2	0.40	1.00	0.10	64.8	47.2	71.6	98.29
3	0.40	0.40	0.00	63.7	47.4	57.0	97.72
4	0.00	1.00	0.10	85.4	57.0	82.0	81.06
5	0.40	0.40	0.10	68.4	27.0	41.3	96.07
6	0.00	0.40	0.00	83.7	75.1	85.8	86.86
7	0.40	1.00	0.00	51.6	57.8	79.0	95.68
8	0.00	0.40	0.10	71.4	56.8	70.0	92.08
9	0.40	1.00	0.00	58.0	55.1	78.5	95.38
10	0.00	1.00	0.10	83.5	49.5	76.0	83.60
11	0.40	0.40	0.10	76.3	49.1	65.7	94.60
12	0.00	0.40	0.00	83.8	75.7	84.3	84.89

Table 2. Central composite design used for the optimization of the responses.

Run	CH % w/v	P % w/v	CMC % w/v	*Y* (%)	*EE* %	Q_{30} (%)	Q_{60} (%)
1	0.60	0.25	0.11	63.78	88.47	40.20	63.30
2	1.00	0.40	0.20	61.58	97.49	43.25	66.72
3	1.00	0.10	0.01	85.58	80.04	56.61	79.31
4	0.20	0.40	0.20	59.85	92.52	21.41	29.51
5	0.60	0.25	0.26	63.70	101.10	49.36	72.25
6	0.10	0.25	0.11	66.91	95.27	27.45	37.69
7	0.60	0.00	0.11	78.73	81.28	56.06	76.85
8	0.60	0.25	0.11	73.94	88.11	43.50	66.20
9	1.00	0.10	0.20	72.28	95.86	49.37	68.08
10	0.60	0.50	0.11	64.97	95.85	31.39	48.95
11	0.60	0.25	0.11	69.88	88.76	35.43	55.43
12	0.60	0.25	0.00	78.18	88.36	50.71	73.90
13	0.20	0.40	0.01	63.36	87.30	50.04	72.30
14	0.20	0.10	0.20	67.55	97.56	21.28	28.24
15	0.20	0.10	0.01	62.27	87.46	76.60	89.50
16	1.27	0.25	0.11	73.99	85.17	41.50	67.50
17	1.00	0.40	0.01	67.29	95.64	52.60	69.20

Determination of ABZ content in microspheres

The *EE* is defined as the percentage of the actual content of drug encapsulated in the polymeric carrier, relative to the initial amount of loaded drug. For the *EE* determination, microspheres were dissolved in 0.1 N HCl for 24 h. The amount of loaded drug was determined by spectrophotometer measurements at 291 nm with a Boeco S-26 spectrophotometer (Hamburg, Germany), according to:

$$EE(\%) = 100 \times (W_{\text{ABZ}}/W_{\text{t}}) \quad (2)$$

where W_{ABZ} is the actual ABZ content and W_{t} is theoretical ABZ content in the microspheres.

Dissolution studies

The microspheres were subjected to dissolution assays in an USP Standard Dissolution Apparatus Hanson Research SR8 Plus (Chatsworth, CA), equipped with a rotational paddle (50 rpm). The dissolution medium (900 mL of 0.1 N HCl) was maintained at 37 °C. Microspheres containing ABZ (100 mg) were introduced into the flasks, and the time counter was set to zero. Samples were measured in triplicate at 10, 30, 60, 90, 120, 180, 240, 300 and 360 min.

Samples of 5 mL were taken using a filter, and the amount of ABZ released was determined. The polymers were found not to interfere with the assay at the working wavelength (291 nm).

An equal volume of the same medium was added to keep a constant volume.

Stability studies

The long-term stability of the microspheres after 14 months at 25 °C was evaluated by means of high-performance liquid chromatography (HPLC) analyses (Hewlett-Packard 1100 Series instrument, equipped with a manual injector, a quaternary pump which includes on line vacuum degasser and a diode array detector). The column used was a LiChroCART® 250-4 LiChrospher® 100 RP-18 (250 × 4 mm I.D, 4 µm).

The methodology was an adaptation of the *European Pharmacopoeia*, 8th ed.[38]. The mobile phase consisting of a solution of ammonium dihydrogen phosphate (1.67 g/L) and methanol at a ratio of 3:7, the flow rate was 0.7 mL/min, the detection wavelength was 254 nm and the injection volume was 20 µL. Under these conditions, the retention time for ABZ was 11.2 min. The linearity was studied at the range between 2 and 100 µg/mL and the correlation coefficients were 0.999. The specificity of the method was evaluated by means of the peak purity determination method using a diode array detector. The microspheres were dissolved in 5 mL of methanol: sulfuric acid (99:1) and diluted to 50.0 mL in the mobile phase.

Evaluation of the microspheres

Morphology by scanning electron microscopy (SEM). Morphology was determined by using SEM in a Leitz SEM AMR 1600 T. Samples were previously sputter-coated with a gold layer in order to make them conductive. The characteristics of the SEM images were analyzed using Image-pro Plus (IPP) software 6.0. About 200 particle diameters were considered in each particle size distribution calculation[39,40].

Determination of bulk density and tapped density. Bulk and tapped density were measured indirectly through the apparent volume, as described in the *European Pharmacopeia*[38]. An accurately weighed quantity of the powder (*W*), was carefully poured into the graduated cylinder and the volume (*Vo*) was measured.

Bulk density (*Dc*) was determined by slowly pouring the samples into a graduated glass cylinder to complete 60% of the container volume. The total volume in bulk density measurements included particle volume, inter-particle void volume and internal pore volume.

Tapped density (*Da*) was determined by applying a controlled packing force to the sample and the interstitial volume and pore volume were included in its calculations. The graduated cylinder was covered with a lid, and placed into the density determination apparatus. The volume (*Vf*) was measured and the operation carried on until two consecutive readings were equal.

Bulk density and tapped density were calculated using the following formulae:

$$\text{Bulk density } (Dc) = W/Vo \tag{3}$$

$$\text{Tapped density } (Da) = W/Vf \tag{4}$$

where *W*: weight of the powder, *Vo*: initial volume and *Vf*: final volume.

Inter-particle porosity (*Ie*) of the particle powder was calculated by the following equation:

$$Ie = (Dc - Da)/(Dc \times Da) \tag{5}$$

Determination of Carr's Index and Hausner ratio

The Carr index (CI%) in the quotient between the bulk and tapped densities expressed as a percentage. The compressibility percentage indirectly gives an idea of the cohesion, size uniformity and surface area of powders[41].

CI was computed from *Da* and *Dc* using the following equation:

$$\text{CI}(\%) = 100 \times (Dc - Da)/Dc \tag{6}$$

The Hausner ratio (*HF*) is the relationship between *Dc* and *Da* and it is related to interparticle friction. It was calculated from *Da* and *Dc* using the following expression:

$$HF = Dc/Da \tag{7}$$

Analysis of angle α

Angle of repose (α) was calculated employing the following equation:

$$\alpha = \tan^{-1} h/r \tag{8}$$

where *h* and *r* were obtained from the three dimensional cone-like pile of the material obtained after the product was passed through a funnel (height 9.5 cm, upper diameter of spout 7.2 cm, internal diameter at the bottom, narrow end of spout 1.8 cm). The funnel was placed on a support at 20 cm from the table surface, centered over a millimeter grid sheet. The narrow end of the funnel spout was plugged and the funnel was filled with the microspheres until it was flushed with the top end of the spout when smoothed with a spatula. Thereafter, the plug was removed and the microspheres were allowed to fall onto the millimeter sheet. The radius of the cone base was measured with a slide caliper and the mean value (*r*) was calculated. Additionally, the cone height (*h*) was measured and finally the angle tangent value (α) of the cone was obtained[38].

Software

The software Design Expert version 7.0.3 (Stat-Ease Inc., Minneapolis, MN) was used to perform the experimental design, polynomial fitting and analysis of variance (ANOVA) study.

Experimental design

An expanded Plackett–Burman design (Table 1) was built in order to estimate the main factors affecting the properties of formulated particles. These factors were evaluated at three levels and a triplicate central point was added to the Plackett–Burman design in order to provide higher information content for the analysis. An ANOVA test was applied to the experimental data corresponding to the design, using the effect of the dummy variables to obtain an estimate of standard errors in the coefficients. After that, a systematic optimization procedure was carried out using response surface methods (RSM), in order to estimate the values of the most important factors leading to the best compromise between maximum responses values. A central composite design was used to apply RSM, in accordance with 17 experiments (combinations of the selected factors) to find the optimal conditions. Finally, a comparison between expected and experimental values obtained with optimized conditions was drawn. Four phases were taken into account to carry out the procedure: (a) screening the influential factors with a Plackett–Burman design, (b) building a response surface model, (c) finding the optimal conditions and (d) experimental verification.

Batch reproducibility

Three batches of the optimal formulation were prepared and their release characteristics were evaluated. *In vitro* release data pertaining to reproducibility studies were compared using $f2$ metric (similarity factor) values[42].

Pharmacokinetic analysis

Animals. The optimized microspheres, the control group (unloaded microspheres) and a suspension of ABZ in distilled water were administrated orally to male Wistar rats (250–300 g) in a single dose. The control group was measured to compare the plasma curves after the oral administration of the three formulations.

The rats were allowed to access to standard laboratory diet and water *ad libitum*, freely prior to the experiment and received care in compliance with international regulations. Experiments with animals were carried out according to the ethical standards formulated in the Declaration of Helsinki, and measures were taken to protect animals from pain or discomfort. The protocol was approved by the Animal Care and Use Committee of the National University of Rosario (Permit Number: 648/2012).

The formulations were administered orally via bucco-gastric tube. Three groups of animals ($n = 3$) were used to evaluate the bioavailability of the formulations. Group 1: ABZ suspended in water, group 2: ABZ microspheres, group 3: unloaded microspheres, as a control group. Each ABZ dosage form was administered at doses of 5 mg/kg. After drug administration, blood samples were collected from the tail vein, at the following time intervals 15, 30, 45, 180, 300, 500 and 1440 min. Lastly, the blood samples were individually heparinized and centrifuged.

Analytical procedure

Samples of plasma were added to 1 mL of methanol (Mallinekradt Chemicals, Milwaukee, WI) in a glass test tube and stored at −20 °C. Residual protein was then separated through centrifugation (12 000 × *g* 4 °C for 12 min).

Samples were concentrated to dryness in a vacuum concentrator and then reconstituted with 500 µL of mobile phase until they were analyzed by a validated HPLC-UV (HPLC Hewlett-Packard 1100) method[43,44].

Samples of 50 µL were injected and the analytes were eluted (flow 1.2 mL/min) from the analytical column using a linear gradient method as reported. The main metabolite, albendazole sulfoxide (ABZSO), was identified by the retention time of pure reference standard. Standards of ABZ and ABZSO were used for the analytical examination of samples.

Bioavailability parameters

The concentration versus time curves for ABZSO in plasma for each individual animal after the different treatments were fitted with PK Solution 2.0 (Summit research services, Ashland, OH). Biexponential concentration–time curves for ABZ after the oral treatment were used.

The peak concentration (C_{max}) and time of peak concentration (T_{max}) were shown in the plotted concentration–time curve of each administered formulation. The $AUC_{0-\infty}$ was calculated as the sum of AUC_{0-24} and $AUC_{24-\infty}$. Also, the AUC_{0-24} was calculated by the trapezoidal rule method and $AUC_{24-\infty}$ was estimated as the quotient between C_{24} and K_e. The K_e value was calculated as a slope, from the final phase of the ln(concentration) − time curves.

Statistical analysis

Results are presented as mean ± SD and the number of animal treated was three for each formulation. Statistical significance of the differences between values was assessed by ANOVA followed by Scheffe's multiple range tests (Stat graphics, Statistical Graphics System, Rockville, MD).

Results and discussion

Screening phase

A satisfactory microspheres formulation depends on many factors; therefore, a Plackett–Burman design was built for estimating the main factors affecting its properties. The analyzed factors were: CH, P and CMC concentrations and its ranges were selected based on prior knowledge about the system under study. The evaluation consisted in analyzing the responses (Y, Q_{30}, Q_{60}, EE and M) in all the conditions are quoted in Table 1. M is a categorical response, and hence values of 1 or 0 were assigned to analyze the morphology: a value of 0 indicates the tendency to form microspheres, while a value of 1 implies a tendency to form microspheres having different non-spherical forms.

Half-normal probability plots for the analyzed responses were built (data not shown) P, CH and CMC concentrations were found to be important factors (values of $p < 0.05$). The responses Y and Q_{30} showed some dependence mainly on the factors P and CMC concentrations. On the other hand, the responses EE and Q_{60} depend mainly on P concentration. Finally, the response M was not significantly influenced by any factor (data not shown). All the microspheres obtained showed a regular morphology which was not included in the optimization process.

Response surface design

Due to the fact that the three selected factors had a significant effect on the responses, a systematic optimization procedure was carried out using RSMs. The aim of this procedure is to estimate the best compromise between maximum dissolution rate at 30 and 60 min, maximum yield and EE. A central composite design was used to apply the RSM, which were combinations of the selected factors in the following ranges: CH concentration from 0.10% to 1.27% w/v, P concentration from 0.10% to 0.50% w/v and CMC concentration from 0.01% to 0.20% w/v (Table 2). All experiments were performed in random order to minimize the effects of uncontrolled factors that may introduce a bias on the measurements.

The responses for all the experiments were fitted to polynomial models, using backward elimination to estimate the best models. These results indicated that a quadratic model better explains the behavior of the responses Q_{30} and Q_{60}, while a linear model is appropriate for EE and Y. A complete ANOVA for the four studied responses is shown in Table 3. Only significant lack of fit was found in EE analysis, which could be explained by the extremely low pure error for this response (Table 3).

The coefficient estimated the uncertainties for the four studied responses and the equations were obtained by means of applying a linear model for the responses Y (Equation (9)) and EE (Equation (10)) or a quadratic model for the responses Q_{30} (Equation (11)) and Q_{60} (Equation (12)) (Table 4). As expected, satisfactory values of the remaining response M were obtained in all runs (as could be anticipated from Plackett–Burman results).

The four responses, as suggested by the analysis of the effect discussed above, were simultaneously optimized (Figure 1): dissolution rate (Q_{30} and Q_{60}), Y and EE which were desirable to be maximum. After the optimization procedure was carried out, a response surface for the global desirability function was built as a function of the influencing factors. The function desirability (D)

Table 3. Complete ANOVA table for the four studied responses.

	Source	Sum of squares	DF*	Mean square	*F* value	Prob > *F*
EE	Model	330.11	2	165.05	9.33	0.0027
	B	97.32	1	97.32	5.50	0.0343
	C	232.80	1	232.80	13.15	0.0027
	Residual	247.79	14	17.70		
	Lack of fit	247.58	12	20.63	194.57	0.0051
	Pure error	0.21	2	0.11		
	Cor total	577.90	16			
Y	Model	523.00	3	174.33	7.86	0.0030
	A	160.95	1	160.95	7.25	0.0184
	B	252.34	1	252.34	11.37	0.0050
	C	109.39	1	109.39	4.93	0.0448
	Residual	288.49	13	22.19		
	Lack of fit	236.19	11	21.47	0.82	0.6672
	Pure error	52.31	2	26.15		
	Cor total	811.49	16			
Q_{30}	Model	2602.78	5	520.56	10.77	0.0006
	A	213.58	1	213.58	4.42	0.0594
	B	444.62	1	444.62	9.20	0.0114
	C	1174.07	1	1174.07	24.29	0.0005
	C^2	583.82	1	583.82	12.08	0.0052
	AC	567.17	1	567.17	11.73	0.0057
	Residual	531.75	11	48.34		
	Lack of fit	498.82	9	55.42	3.37	0.2499
	Pure error	32.92	2	16.46		
	Cor total	3134.53	16			
Q_{60}	Model	4020.98	5	804.20	11.62	0.0004
	A	901.51	1	901.51	13.02	0.0041
	B	402.61	1	402.61	5.81	0.0345
	C	1510.53	1	1510.53	21.82	0.0007
	C^2	659.43	1	659.43	9.52	0.0104
	AC	1020.16	1	1020.16	14.73	0.0028
	Residual	761.61	11	69.24		
	Lack of fit	699.49	9	77.72	2.50	0.3181
	Pure error	62.11	2	31.06		
	Cor total	4782.59	16			

*DF, degrees of freedom.

ranges from 0 (value totally undesirable) to 1 (all responses are in a desirable range simultaneously) and is defined by Equation (13), where *d*1, *d*2, . . ., *dN* correspond to the individual desirability function for each response being optimized:

$$D = \left[\prod_{n=1}^{N} (d_n)^{\mathrm{wn}}\right] 1/\Sigma wn_{n=1}^{N} \quad (13)$$

where *wn* is a weight which controls the relative importance of each of the analyzed factors. In the present work, all weights were set to unity, so, a simplified version of Equation (14) was employed.

$$D = \left[\prod_{n=1}^{N} d_n\right]^{1/N} \quad (14)$$

The optimal conditions were found to be: CH concentration, 1.00% w/v, P concentration 0.10% w/v and CMC concentration 0.20% w/v.

As can be seen in Figure 1, lower P concentrations and higher CH concentrations produced faster dissolution rates and higher *Y*. However, better *EE* values were obtained at higher P concentrations but lower CH concentrations. The *EE* was increased when CMC was employed at higher concentrations, but better values of *Y* and dissolution rate were obtained at low CMC concentrations. It is important to highlight that the evident competition between CMC and P to achieve a better ionic interaction with CH governs the dissolution behavior.

Therefore, we chose as the best conditions those corresponding to the design point, which were closer to the region suggested by the desirability function. The desirability function at this point yields a value of $D = 0.64$, which we consider to be adequate for our purposes.

Experimental verification

The optimal conditions for the preparation of microspheres were verified by independent additional experiment. The experimental results were in agreement with the target values, and the

Table 4. Coefficient estimates and their uncertainties for the four studied responses.

	Factor	Coefficient estimate	DF*	Standard error	Final equation in terms of coded factors
Y	Intercept	69.06	1	1.14	$Y = 69.06 + 3.61{*}A - 4.31{*}B - 3.02 \times C$ Equation (9)
	A	3.61	1	1.34	
	B	−4.31	1	1.28	
	C	−3.02	1	1.36	
EE	Intercept	90.80	1	1.02	$EE = 90.80 + 2.67{*}B + 4.40\ {*}C$ Equation (10)
	B	2.67	1	1.14	
	C	4.40	1	1.21	
Q_{30}	Intercept	38.19	1	2.40	$Q_{30} = 38.19 + 4.16{*}A - 5.72{*}B - 10.32{*}C + 8.44{*}C^2 + 8.42{*}AC$ Equation (11)
	A	4.16	1	1.98	
	B	−5.72	1	1.88	
	C	−10.32	1	2.09	
	C^2	8.44	1	2.43	
	AC	8.42	1	2.46	
Q_{60}	Intercept	56.47	1	2.87	$Q_{60} = 56.47 + 8.54{*}A - 5.44{*}B - 11.70{*}C + 8.97{*}C^2 + 11.29{*}AC$ Equation (12)
	A	8.54	1	2.37	
	B	−5.44	1	2.26	
	C	−11.70	1	2.51	
	C^2	8.97	1	2.91	
	AC	11.29	1	2.94	

*DF, degrees of freedom.

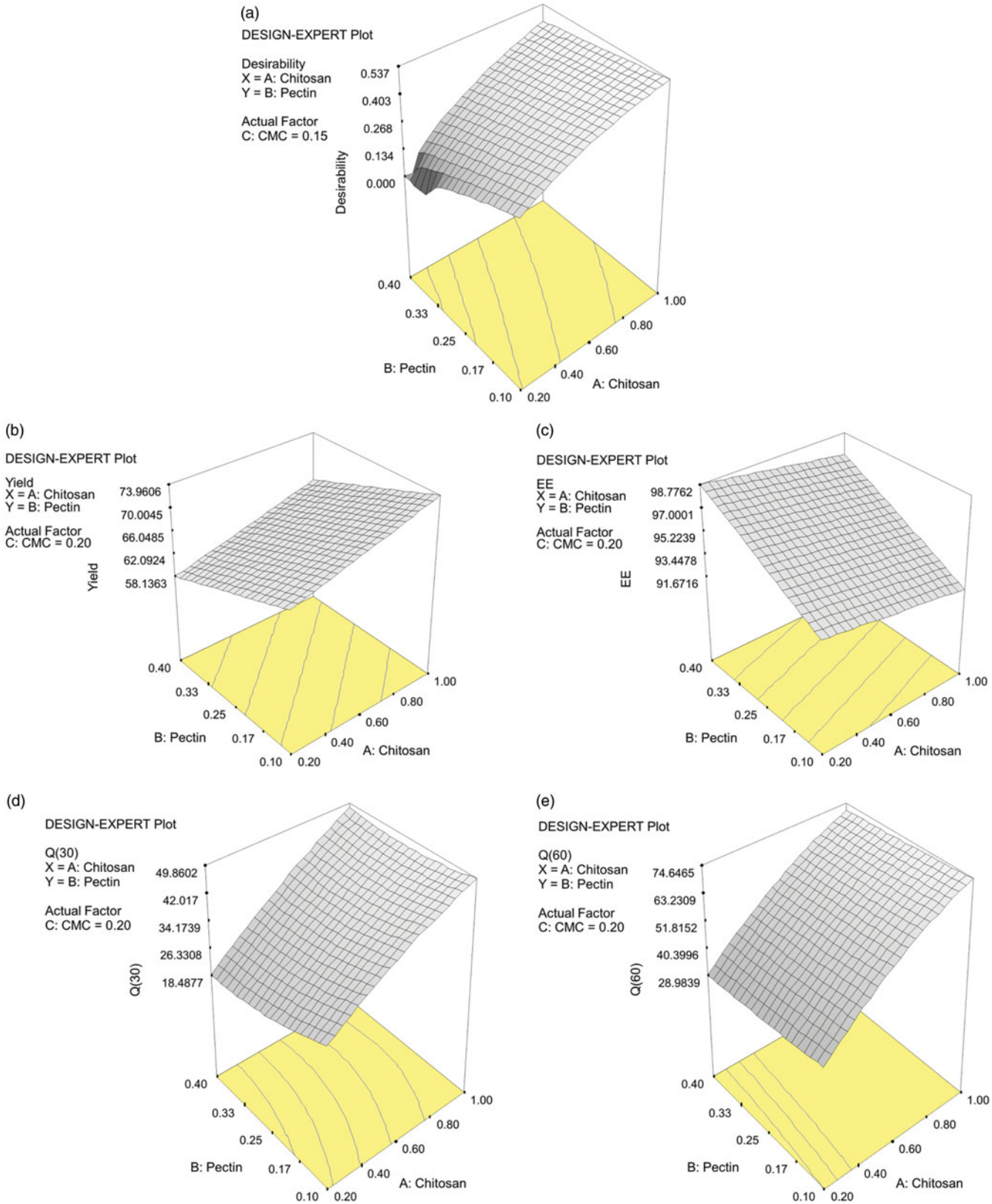

Figure 1. Response surface plots for the global desirability function (a), yield (b), *EE* (c), Q_{30} (d) and Q_{60} (e) as indicated.

differences found are within the range of the analytical measurement error (Table 5).

The dissolution profile for a formulation obtained in the selected conditions was contrasted with untreated ABZ (Figure 2a). As can be seen, the microspheres formulation showed an enhanced dissolution rate for ABZ, in comparison with the untreated drug. Microspheres obtained in the optimal conditions have spherical shape. The shape and surface morphology of the microspheres were observed by SEM (Figure 2b). The mean diameter was 2.8 μm ± SD 1.9, the minimum particle size observed was 0.8 μm and the maximum particle size was 10.7 μm[39,40].

Batch reproducibility

Three batches of the optimal formulation were prepared and the dissolution rate was performed as previously described in section ''Dissolution studies''. No significant differences were observed in the release profiles of the formulations between different batches, as indicated by *f*2 metric (similarity factor). The obtained *f*2 values were 76.75, 64.04 and 61.94. Due to the fact that *f*2 values higher than 50% showed no significant differences between batches, this study indicated that the formulation methodology employed was found to be suitable for formulation of ABZ microspheres.

Stability studies

Stability studies were performed for the optimal microsphere formulation after 14 months. Microspheres were stored in glass bottles at room temperature (25 °C) and evaluated for any change in shape and structural integrity by microscopic examination and residual drug content.

The results revealed that no considerable changes in shape and, thus, no significant differences in drug content were observed. The mean ABZ content was $96 \pm 1\%$ at 25 °C.

Microspheres characterization, evaluation and flow properties

The results were obtained in triplicate in accordance with the described methodology. The values for the microspheres were: $Da = 0.338$; $Dc = 0.575$; $Ie = 1.214$; CI = 41.16; $HF = 1.698$ and, finally, the angle of repose $\alpha = 38.48$. These parameters indicate that microspheres presented poor compressibility and flow properties, clearly indicated by the relationship between CI and α. Additionally, the *HF* results suggested a high cohesive and an inadequate flow behavior. Therefore, in order to be able to formulate a suitable blend, one or more excipients must be added to improve the poor indices and parameters.

Table 5. Comparison between expected and experimental values obtained with optimized conditions.

Response	Predicted value	Experimental value
Yield (%)	73.96	74.04
Encapsulation efficiency (%)	91.67	92.09
Dissolution rate (Q_{30})	49.86	44.16
Dissolution rate (Q_{60})	74.65	67.55

Pharmacokinetics studies

The bioavailability of the ABZ-loaded microspheres was evaluated. The pharmacokinetics data are shown in Figure 3. ABZ, as a parent drug, was not detected in plasma. ABZSO, the active metabolite, was detected in plasma during 1440 min (24 h). The studies did not reveal significant results with the control group. Microspheres obtained under the optimal conditions showed a better $AUC_{0-\infty}$ in comparison with the unloaded drug. Clearly, a significant increase in the AUC data was obtained with the novel formulation. The optimized microspheres showed an AUC almost 10 times higher than the pure drug and the C_{max} was 1274 ng/mL, in comparison with the C_{max} obtained by the oral administration of ABZ without any treatment was 179 ng. The T_{max} observed after 300 min of the oral dose was remarkably modified, in comparison with the pure drug. In accordance with the dissolution profiles performed (Figure 2a), as described by Dib et al.[43], the rate of dissolution of ABZ in the gastrointestinal tract was thought to be extremely important in achieving adequate absorption and the consequent availability. The ABZ formulations must dissolve at the stomach pH. The comparative plasma pharmacokinetic plots revealed substantial increased concentrations and AUC values after the oral administration of the microsphere formulations. This novel formulation could contribute to evaluate anthelmintic activity, with improved absorption parameters. The results clearly showed the advantages of administrating oral microparticulate system in comparison with the aqueous suspension of ABZ to improve the therapeutic alternatives to treat some helminthiasis.

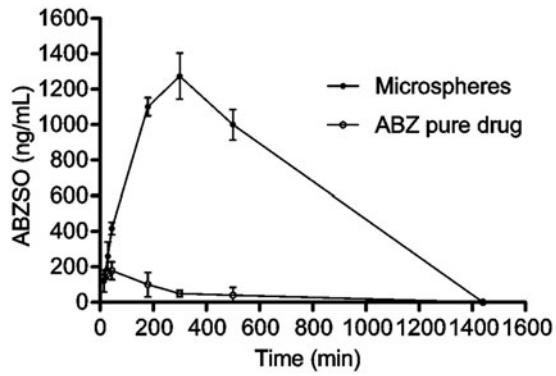

Figure 3. Plasma concentration of ABZSO after the oral administration of ABZ (pure drug), and the optimized ABZ microspheres.

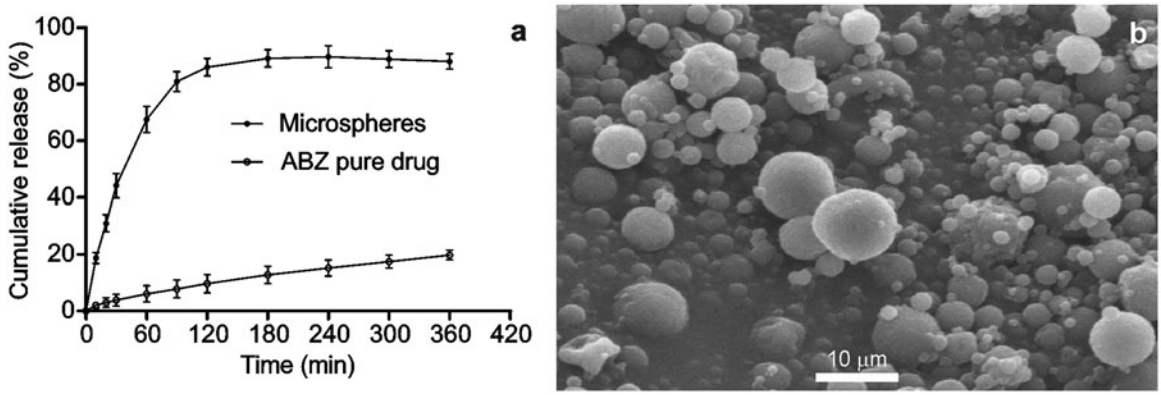

Figure 2. (a) Dissolution profile of 100 mg ABZ pure drug and the same dosage prepared according to optimized ABZ microspheres. (b) Scanning electron microscopy (SEM) ABZ microspheres.

Conclusions

This experimental design approach could be successfully used in the development of microsphere formulations of ABZ with predictable morphology, entrapment efficiency, yield and drug release properties. Particularly, the experimental design allowed the simultaneous evaluation, by a response surface study, of the effects of the selected variables: % of the ionic polymers (CH, P and CMC concentrations) on five responses: the yield (Y), morphology (M), dissolution rate at 30 (Q_{30}) and 60 (Q_{60}) min and EE. The optimal conditions were found to be: CH concentration, 1.00% w/v, P concentration 0.10% w/v and CMC concentration 0.20% w/v. The experimental values of the responses obtained from the optimized microsphere formulations were very close to the predicted values, demonstrating the actual reliability and usefulness of the assumed model in the preparation of ABZ microspheres with optimized and predictable properties, suitably adaptable to obtain the desired drug release profile. It can be expected that this application of experimental design tools could be useful for further formulation studies, where microspheres with different drug release profiles could be required.

Acknowledgements

We would like to thank Marcela Culasso, María Robson, Mariana de Sanctis and Geraldine Raimundo for their assistance in the correction of the language.

Declaration of interest

The authors report no conflicts of interest. The authors alone are responsible for the content and writing of this article.

A.G. and G.P. are grateful to CONICET for a Doctoral and a Post-Doctoral Fellowship. The University of Rosario, CONICET (Consejo Nacional de Investigaciones Científicas y Técnicas, Project No. PIP 112-201001-00194) and ANPCyT (Agencia Nacional de Promoción Científica y Tecnológica, Project No. PICT 2006-1126) are gratefully acknowledged for financial support.

References

1. Herrero EP, Valle EMMD, Galán MA. Development of a new technology for the production of microcapsules based in atomization processes. Chem Eng J 2006;117:137–42.
2. Sandri G, Bonferoni MC, Chetoni P, et al. Ophthalmic delivery systems based on drug–polymer–polymer ionic ternary interaction: in vitro and in vivo characterization. Eur J Pharm Biopharm 2006; 62:59–69.
3. Quinteros DA, Rigo VR, Kairuz AFJ, et al. Interaction between a cationic polymethacrylate (Eudragit E100) and anionic drugs. Eur J Pharm Sci 2008;33:72–9.
4. Lankalapalli S, Kolapalli RM. Biopharmaceutical evaluation of diclofenac sodium controlled release tablets prepared from gum karaya-chitosan polyelectrolyte complexes. Drug Dev Ind Pharm 2012;38:815–24.
5. Wang FQ, Li P, Zhang JP, et al. A novel pH-sensitive magnetic alginate-chitosan beads for albendazole delivery. Drug Dev Ind Pharm 2010;36:867–77.
6. Liu YH, Zhu X, Zhou D, et al. pH-sensitive and mucoadhesive microspheres for duodenum-specific drug delivery system. Drug Dev Ind Pharm 2011;37:868–74.
7. Rozenberg BA, Tenne R. Polymer-assisted fabrication of nanoparticles and nanocomposites. Prog Polym Sci 2008;33:40–112.
8. Dreve S, Kacso I, Popa A, et al. Structural investigation of chitosan-based microspheres with some anti-inflammatory drugs. J Mol Struct 2011;997:78–86.
9. Lu Z, Chen W, Hamman JH. Chitosan-polycarbophil interpolyelectrolyte complex as a matrix former for controlled release of poorly water-soluble drugs I: *in vitro* evaluation. Drug Dev Ind Pharm 2010;36:539–46.
10. El-Gibaly I, Meki AMA, Abdel-Ghaffar SK. Novel B melatonin-loaded chitosan microcapsules: in vitro characterization and antiapoptosis efficacy for aflatoxin B1-induced apoptosis in rat liver. Int J Pharm 2003;260:5–22.
11. Zhang Y, Wei W, Lv P, et al. Preparation and evaluation of alginate–chitosan microspheres for oral delivery of insulin. Eur J Pharm Biopharm 2011;77:11–19.
12. Xu Q, Xia Y, Wang C-H, Pack DW. Monodisperse double-walled microspheres loaded with chitosan-p53 nanoparticles and doxorubicin for combined gene therapy and chemotherapy. J Control Release 2012;163:130–5.
13. Pillai CKS, Paul W, Sharma CP. Chitin and chitosan polymers: chemistry, solubility and fiber formation. Prog Polym Sci 2009;34: 641–78.
14. Kasaai MR. A review of several reported procedures to determine the degree of N-acetylation for chitin and chitosan using infrared spectroscopy. Carbohyd Polym 2008;71:497–508.
15. Liu Y, Tang J, Chen X, Xin JH. A templating route to nanoporous chitosan materials. Carbohyd Res 2005;340:2816–20.
16. Felt O, Buri P, Gurny R. Chitosan: a unique polysaccharide for drug delivery. Drug Dev Ind Pharm 1998;24:979–93.
17. Marudova M, Lang S, Brownsey GJ, Ring SG. Pectin-chitosan multilayer formation. Carbohydr Res 2005;340:2144–9.
18. Marudova M, MacDougall AJ, Ring SG. Pectin-chitosan interactions and gel formation. Carbohydr Res 2004;339:1933–9.
19. Lin Y, Chen Q, Luo H. Preparation and characterization of N-(2-carboxybenzyl)chitosan as a potential pH-sensitive hydrogel for drug delivery. Carbohyd Res 2007;342:87–95.
20. Zambito Y, Di Colo G. Preparation and in vitro evaluation of chitosan matrices for colonic controlled drug delivery. J Pharm Pharm Sci 2003;6:274–81.
21. Yu CY, Yin BC, Zhang W, et al. Composite microparticle drug delivery systems based on chitosan, alginate and pectin with improved pH-sensitive drug release property. Colloid Surface B 2009;68:245–9.
22. Kas HS. Chitosan: properties, preparations and application to microparticulate systems. J Microencapsul 1997;14:689–711.
23. Itoh K, Hirayama T, Takahashi A, et al. In situ gelling pectin formulations for oral drug delivery at high gastric pH. Int J Pharm 2007;335:90–6.
24. Gómez-Burgaz M, García-Ochoa B, Torrado-Santiago S. Chitosan–carboxymethylcellulose interpolymer complexes for gastric-specific delivery of clarithromycin. Int J Pharm 2008;359:135–43.
25. Lü S, Liu M, Ni B. An injectable oxidized carboxymethylcellulose/N-succinyl-chitosan hydrogel system for protein delivery. Chem Eng J 2010;160:779–87.
26. Kawabata Y, Wada K, Nakatani M, et al. Formulation design for poorly water-soluble drugs based on biopharmaceutics classification system: basic approaches and practical applications. Int J Pharm 2011;420:1–10.
27. Castillo JA, Palomo-Canales J, Garcia JJ, et al. Preparation and characterization of albendazole beta-cyclodextrin complexes. Drug Dev Ind Pharm 1999;25:1241–8.
28. Dayan AD. Albendazole, mebendazole and praziquantel. Review of non-clinical toxicity and pharmacokinetics. Acta Trop 2003;86: 141–59.
29. Vogt M, Kunath K, Dressman JB. Dissolution improvement of four poorly water soluble drugs by cogrinding with commonly used excipients. Eur J Pharm Biopharm 2008;68:330–7.
30. Simi SP, Saraswathi R, Sankar C, et al. Formulation and evaluation of albendazole microcapsules for colon delivery using chitosan. Asian Pac J Trop Med 2010;3:374–8.
31. Daniel-Mwambete K, Torrado S, Cuesta-Bandera C, et al. The effect of solubilization on the oral bioavailability of three benzimidazole carbamate drugs. Int J Pharm 2004;272:29–36.
32. Sinha VR, Singla AK, Wadhawan S, et al. Chitosan microspheres as a potential carrier for drugs. Int J Pharm 2004;274:1–33.
33. Stulzer HK, Tagliari MP, Parize AL, et al. Evaluation of cross-linked chitosan microparticles containing acyclovir obtained by spray-drying. Mater Sci Eng B 2009;29:387–92.
34. Lee J-S, Kim JS, Lee HG. γ-Oryzanol-loaded calcium pectinate microparticles reinforced with chitosan: optimization and release characteristics. Colloid Surface B 2009;70:213–17.
35. Leonardi D, Lamas MC, Olivieri AC. Multiresponse optimization of the properties of albendazole–chitosan microparticles. J Pharm Biomed Anal 2008;48:802–7.
36. Swain S, Behera UA, Beg S, et al. Design and characterization of enteric-coated controlled release mucoadhesive

microcapsules of Rabeprazole sodium. Drug Dev Ind Pharm 2013;39:548–60.
37. Piccirilli G, García A, Leonardi D, et al. Chitosan microparticles: influence of the gelation process on the release profile and oral bioavailability of albendazole, a class II compound. Drug Dev Ind Pharm 2013. [Epub ahead of print]. doi:10.3109/03639045.2013.829486.
38. European Pharmacopoeia. 8th ed. Strasbourg, France; 2013.
39. Tansel B, Nagarajan P. SEM study of phenolphthalein adsorption on granular activated carbon. Adv Environ Res 2004;8:411–15.
40. Adami R, Reverchon E. Composite polymer-Fe_3O_4 microparticles for biomedical applications, produced by Supercritical Assisted Atomization. Powder Technol 2012;218:102–8.
41. Singh I, Kumar P. Preformulation studies for direct compression suitability of cefuroxime axetil and paracetamol: a graphical representation using SeDeM diagram. Acta Pol Pharm 2012;69:87–93.
42. Costa P, Sousa Lobo JM. Modeling and comparison of dissolution profiles. Eur J Pharm Sci 2001;13:123–33.
43. Dib A, Palma S, Suarez G, et al. Albendazole sulphoxide kinetic disposition after treatment with different formulations in dogs. J Vet Pharmacol Ther 2011;34:136–41.
44. Kitzman D, Cheng KJ, Fleckenstein L. HPLC assay for albendazole and metabolites in human plasma for clinical pharmacokinetic studies. J Pharm Biomed Anal 2002;30:801–13.